

Cornell fast rotation Fourier method

A. Chapelain¹, J. Fagin¹, D. Rubin¹, and D. Seleznev¹

¹Cornell University

Abstract

This note presents the details of the Cornell fast rotation Fourier method. This method aims at reconstructing the radial distribution of the stored muon beam, via reconstructing the frequency distribution, in order to estimate the electric field correction to the anomalous spin precession frequency of the muon ω_a .

Contents

1	Introduction	2
2	Fast rotation signal	3
3	Producing the fast rotation signal	5
3.1	Positron counts	5
3.2	Calorimeters combination	5
3.3	Wiggle fit	6
4	Fourier method	9
5	Background correction	14
5.1	Signal and background	14
5.2	Background correction	14
6	t_0 optimization	17
6.1	Why optimizing?	17
6.2	Optimization procedure	20
6.2.1	First iteration	20
6.2.2	Next iterations	21

7	t_s and t_m optimization	22
7.1	Spectral leakage	22
7.2	t_s optimization	22
7.3	t_m optimization	23
8	Frequency to radius conversion	26
9	Performance study and Run-1 data analysis	27
10	Analysis code	28

1 Introduction

This note presents the details of the Cornell fast rotation Fourier method. This method aims at reconstructing the radial distribution of the stored muon beam, via reconstructing the frequency distribution, in order to estimate the electric field correction to the anomalous spin precession frequency of the muon ω_a . The electric field correction C_E can be estimated in first approximation with the following formula:

$$C_E = \frac{\Delta\omega_a}{\omega_a} = -2n(1-n)\beta^2 \frac{\langle x_e^2 \rangle}{R_0^2}, \quad (1)$$

where

$$\langle x_e^2 \rangle = x_e^2 + \sigma^2, \quad (2)$$

where x_e is the equilibrium radius of the beam (its average radial position) and σ is its width. R_0 is the magic radius of 7112 mm, β the relativistic speed, and n the field index that relates to the electrostatic quadrupole electric field gradient like:

$$n = \frac{m\gamma r}{pB_0} \frac{\partial E_r}{\partial r}, \quad (3)$$

where m mass, γ the Lorentz factor, r the radial distance from the center of the storage ring, p the momentum, and E_r the radial component of the quadrupole electric field.

This goal of the Fermilab E-989 is an uncertainty budget on the electric field correction of 20 ppb. This uncertainty translates into knowing both the average and the width of the cyclotron revolution frequency distribution to couple 0.1 kHz, which corresponds to knowing both the equilibrium radius and the width of the radial distribution to couple 0.1 mm.

The fast rotation Fourier method was first developed for the BNL E-821 experiment [1]. We re-derived the method from first principles for the Fermilab E-989 experiment in order to

thoroughly understand and expand it [2]. The note [2] also introduces the need for the electric field correction along with explaining what is the fast rotation signal and how it allows to reconstruct the radial distribution. Therefore these topics will be re-introduced only briefly. This note will focus on presenting the Cornell implementation of the fast rotation Fourier method that goes beyond the BNL method.

2 Fast rotation signal

Fast rotation refers to the cyclotron motion of the muon beam in the storage ring with a revolution frequency of 6.705 MHz (period of 149.14 ns) for muons traveling on the so-called “magic orbit” (radius of 7112 mm) with the so-called “magic momentum” (3.094 GeV/c). The muon beam is injected bunched into the ring. The longitudinal width of the stored beam is shorter than the cyclotron revolution period, i.e., the beam does not fill the full azimuth of the ring. This feature allows to reconstruct a periodic signal as seen by a given detector at a fixed location. This detector sees the beam intensity modulates as the beam goes around the ring. The beam eventually debunches after dozens of micro-seconds. The debunching is mainly due to the momentum spread of the stored beam: different momenta result in different radii thus different revolution periods/frequencies. The periodicity of the fast rotation signal allow to reconstruct the radial distribution of the stored beam. Section 2 of [2] provides more details about the fast rotation.

The anomalous spin precession frequency ω_a of the stored muons is measured from the decay positrons information made available by 24 electromagnetic calorimeters located on the inner side of the storage ring. Therefore, the fast rotation signal of interest to estimate the electric field contribution to ω_a is the one measured by the calorimeters. The calorimeters signals correspond to the positron counts as a function of time $N(t)$. This signal exhibits features originating from beam dynamics, calorimeter acceptance and the anomalous spin precession. These features need to be corrected for in order to retrieve a pure enough fast rotation signal that has to do only with the cyclotron motion of the beam. The lack of correction would drastically reduce the performance of the fast rotation method. The correction is performed dividing the fast rotation signal by a fit to the data that includes the features to be factored out. The simplest fit to the data is the standard 5-parameter fit:

$$N(t) = N_0 e^{-t/\tau} [1 + A \cos(\omega_a t + \phi)], \quad (4)$$

where N_0 is the number of detected positron at $t = 0 \mu s$, τ is the muon boosted life-time of about $64 \mu s$, A called the asymmetry is the amplitude of the modulation due to the spin precession, ω_a the anomalous spin precession frequency (or spin tune) and ϕ the phase of the modulation. Figure 1 shows an example of a pure fast rotation period generated by a

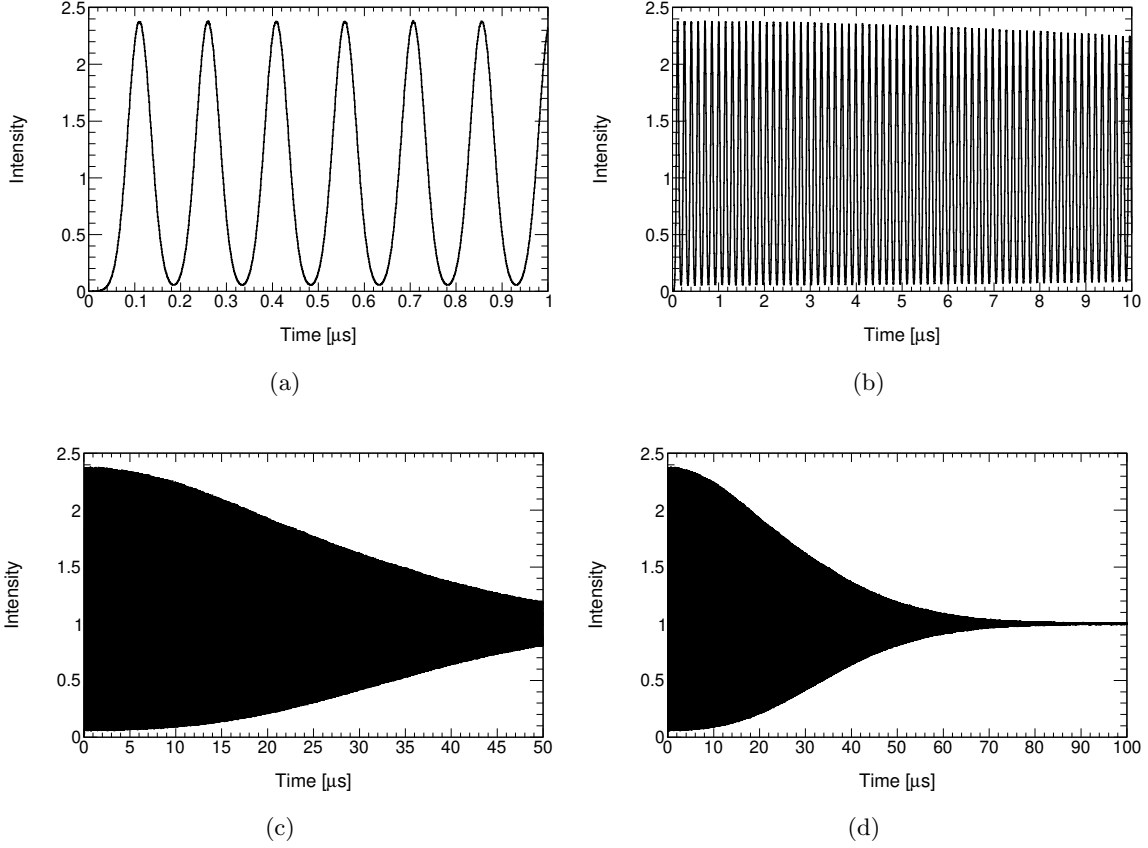


Figure 1: Fast rotation signal as a function of time generated by a toy Monte Carlo [3]. This simulated signal has a Gaussian frequency/momentum distribution with a width (one standard deviation) of 0.09% (6 kHz/0.003 GeV/c), a Gaussian initial longitudinal beam profile with a width (one standard deviation) of 25 ns and zero emittance (no transverse beam size). Four time intervals are shown: (a) 0-1 μ s, (b) 0-10 μ s, (c) 0-50 μ s, (d) 0-100 μ s with respect to the beam injection.

toy Monte Carlo [3]. Section 3 will detail further the procedure to produce the fast rotation signal using experimental data

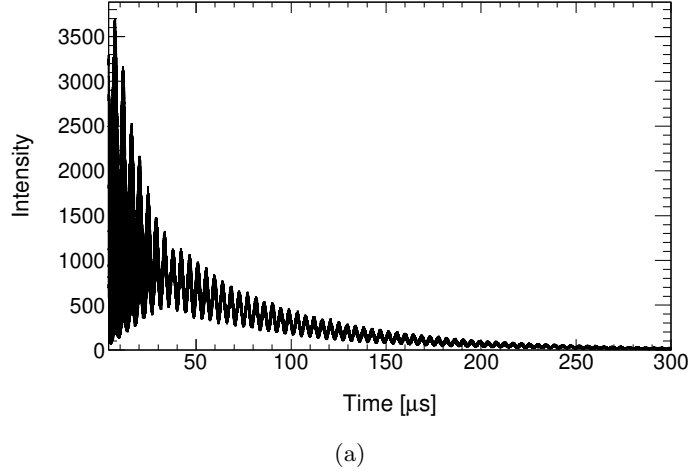


Figure 2: Positron counts as a function of time as seen by calorimeter #1 for the Run-1 60-hour data set for the time range 4-300 μs with respect to the beam injection. The time interval is 1 ns.

3 Producing the fast rotation signal

3.1 Positron counts

Figure 2 shows the positron counts as a function of time as measured by calorimeter #1 for the Run-1 60-hour data set. This spectrum clearly exhibits the exponential muon decay with a boosted life-time of about 64 μs and the anomalous spin precession modulation ω_a . There are other features one cannot see without thorough fitting studies such as: coherent betatron motion, vertical waist motion, muon loss, pile-up, gain variation. These studies are central to the measurement of the anomalous precession frequency ω_a and are beyond the scope and needs of the fast rotation analysis.

3.2 Calorimeters combination

The first step to produce the fast rotation signal is to combine the signals from the 24 calorimeters together to maximize the statistics¹. The combination is performed adding all the positron counts spectra together time shifting 23 of them with respect to the 24th taken as the reference calorimeter (arbitrarily chosen as calorimeter #1). The time shift is initially set to one 24th of the nominal cyclotron revolution period (the so-called “magic” cyclotron revolution period of 149.14), i.e., 6.214 ns. Once the first round of the fast rotation analysis is complete, the time shift value is updated using the measured cyclotron revolution period

¹The analysis is also performed calorimeter-by-calorimeter as a check that the results are uniform around the ring.

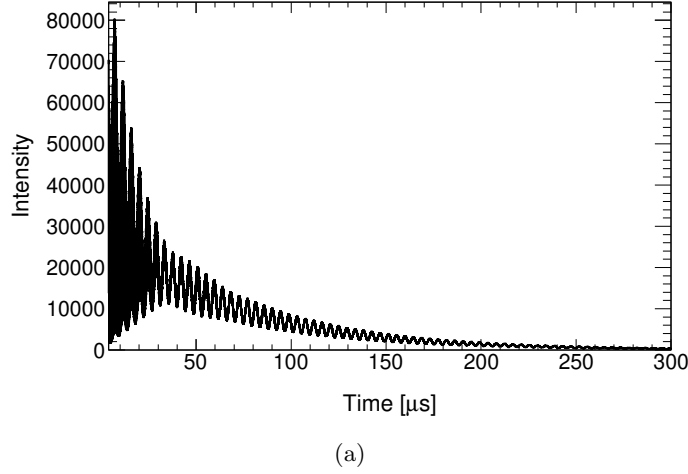


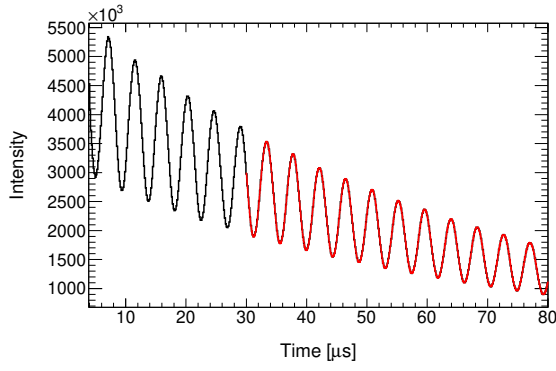
Figure 3: Positron counts as a function of time as seen by all the calorimeters combined for the Run-1 60-hour data set for the time range 4-300 μs with respect to the beam injection. The time interval is 1 ns.

and the analysis is performed again. It should be noted that the small allowed range of variation in the cyclotron revolution period does not lead to any sizable difference in the fast rotation analysis results. Figure 3 shows the positron counts as a function of time for all the calorimeters combined together with calorimeter #1 as the reference.

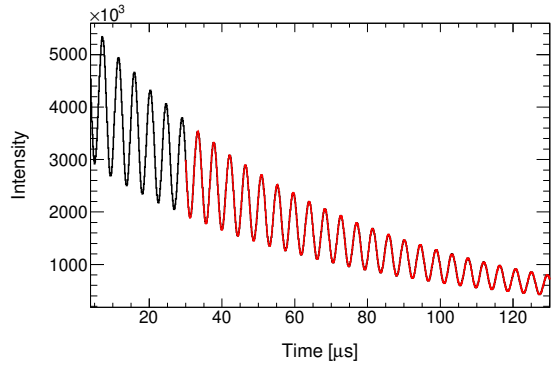
3.3 Wiggle fit

The second step requires to fit the combined spectrum to factor out the two most prominent features: muon life-time and anomalous precession modulation ω_a . To do so, the spectrum is re-binned from its nominal time bin interval of 1 ns to 149 ns in order to average out in first order the cyclotron motion. This re-binning facilitate the fitting procedure. The re-binned spectrum is fitted using the standard 5-parameter fit or 9-parameter fit. The original 1 ns time interval spectrum is then divided, given proper normalization, by the fit function in order to produce the fast rotation signal that only exhibits the cyclotron modulation with an average intensity of 1. This spectrum is the input to the fast rotation Fourier method.

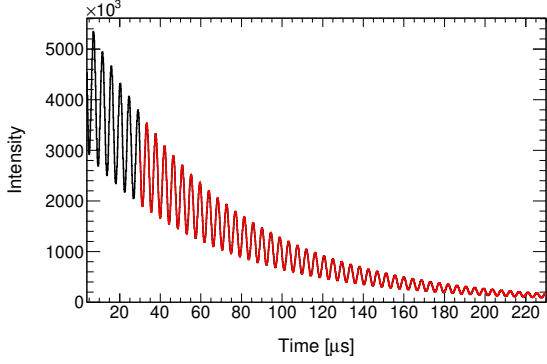
Figure 4 shows the 9-parameter fit to the combined calorimeters spectrum for the Run-1 60-hour data set. Figure 5 shows the resulting fast rotation signal after correcting the positron counts spectrum using its 9-parameter fit. The importance of the the number of fit parameters will be investigated as a source of systematic uncertainty in analyzing the Run-1 data set [4, 5, 6, 7].



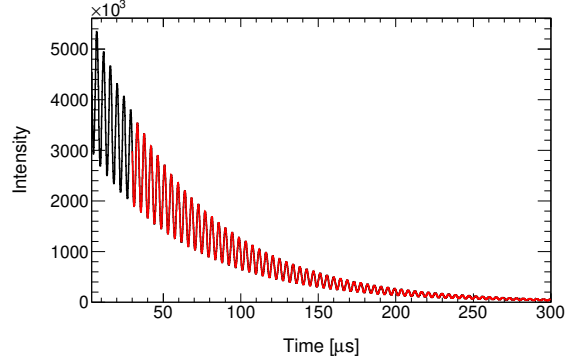
(a)



(b)

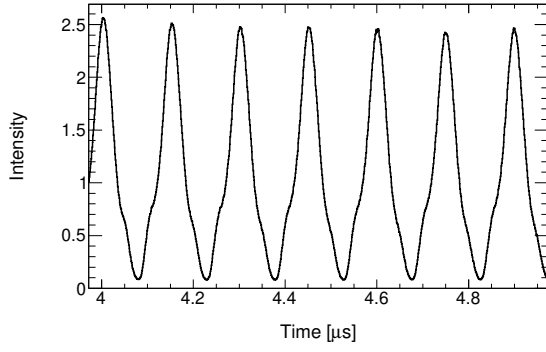


(c)

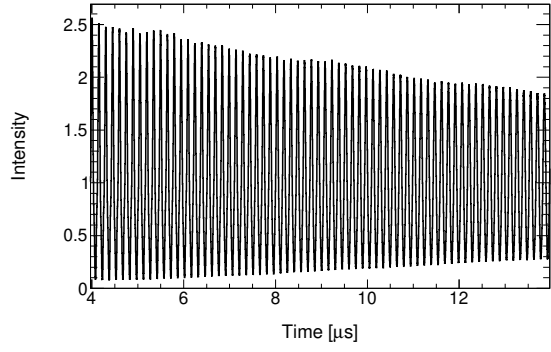


(d)

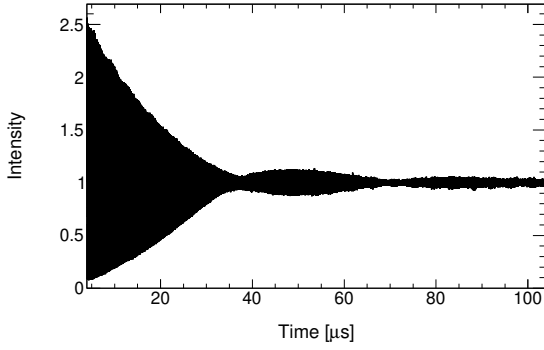
Figure 4: 9-parameter wiggly fit to the combined calorimeters spectrum for the Run-1 60-hour data set for the time ranges: (a) 4-80, (b) 4-130, (c) 4-230, (d) 4-300 μs with respect to the beam injection. The start time of the fit is 30 μs . The time interval is 149 ns.



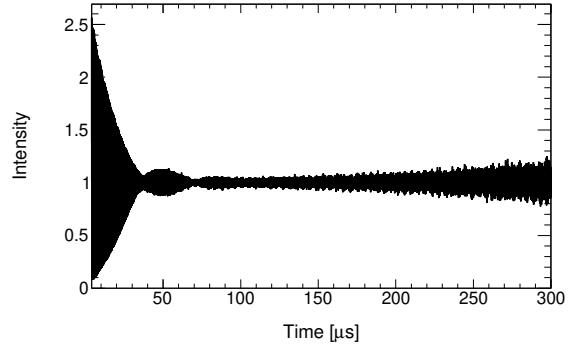
(a)



(b)



(c)



(d)

Figure 5: Fast rotation signal of the combined calorimeters spectrum for the Run-1 60-hour data set for the time ranges: (a) 4-5, (b) 4-14, (c) 4-104, (d) 4-300 μs with respect to the beam injection. The time interval is 1 ns.

4 Fourier method

The muon storage ring is a weak focus ring. This leads to a straightforward frequency–radius equivalence that allows to convert in a simple fashion from one to the other (see Sec. 8). The Fourier method takes advantage of this equivalence as well as the fact that the beam is injected bunched into the ring and remains bunched for dozens of micro-seconds. This periodic signal allows to reconstruct the frequency distribution of the stored beam and therefore the radial distribution.

The Fourier method relies on calculating the cosine Fourier transform² (the real part of the Fourier transform) of the fast rotation signal [2]:

$$S(\omega, t_s, t_m) = \int_{t_s}^{t_m} S(t) \cos[\omega(t - t_0)] dt, \quad (5)$$

where $S(t)$ is the fast rotation signal, t_0 the time corresponding to the center of mass of the beam passing the detector for the first time (first turn), and t_s and t_m are respectively the start and end time of the fast rotation signal with respect to the beam injection. The parameter t_0 , t_s and t_m are at the core of the Fourier analysis. In the ideal case of $t_s = t_0$, meaning having access to the data from injection, i.e., from the first turn when the muon beam enters the ring, eq. (5) is exact and yields the correct frequency distribution $\Phi(\omega)$:

$$\Phi(\omega) = S(\omega, t_s = t_0, t_m) = \int_{t_0}^{t_m} S(t) \cos[\omega(t - t_0)] dt. \quad (6)$$

Figure 6 shows the good agreement between the truth-level frequency distribution and the cosine Fourier transform using toy Monte Carlo simulation [3].

²The simplest derivation of the formula requires a symmetric incoming longitudinal beam profile as shown in [2] Sec. 3.3. It was shown though, in [2] Sec 3.4, that this assumption is not required. Asymmetric beam profile do not decrease the performance of the method.

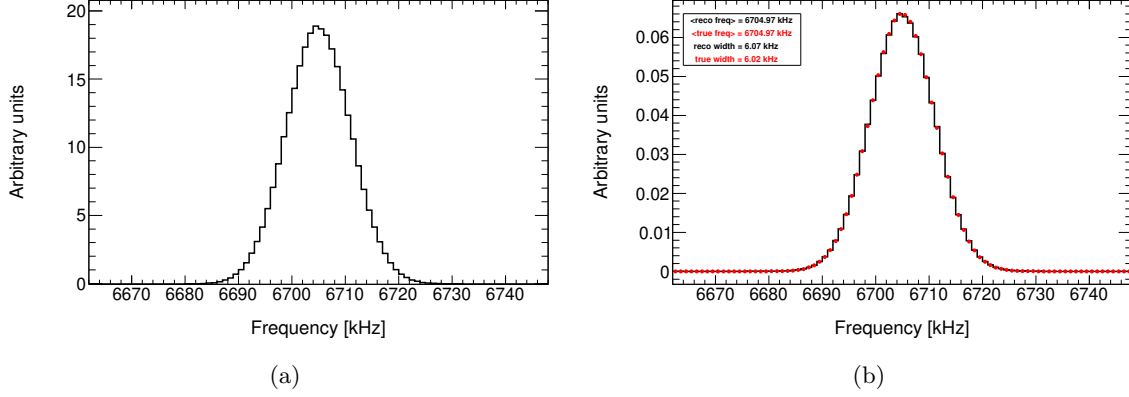


Figure 6: Frequency distributions: (a) cosine Fourier transform for $t_s = t_0$, (b) overlay of the cosine Fourier transform (black) with the truth-level distribution (red) for $t_s = t_0$. The analyzed fast rotation signal originates from the toy Monte Carlo simulation [3].

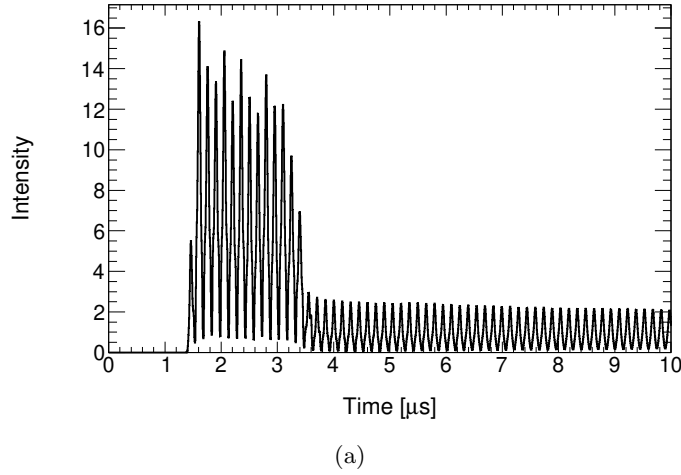


Figure 7: Fast rotation signal for the combined calorimeters for the 60-hour data set for the time range 0-10 μs . The fast rotation signal stabilizes at about 4 μs after injection. The calorimeters data up to 1.2 μs is not recorded. Beam-line positrons contaminate the muon beam until about 4 μs after injection.

Unfortunately, as can be seen in Fig. 7, the calorimeter data for Run-1 appears stable only about 4 μ s after injection due to detector saturation and positron beam-line contamination. Given that t_0 is about 0.1 μ s, and therefore $t_s \gg t_0$, the cosine Fourier transform of eq. (5) is only an approximation of the frequency distribution. It requires the following correction term [2, 8]:

$$\Delta(\omega) = \int_{\omega^-}^{\omega^+} S(\omega') \frac{\sin [(\omega - \omega')(t_s - t_0)]}{\omega - \omega'} d\omega'. \quad (7)$$

The correct frequency distribution can be retrieved correcting the cosine Fourier transform given the relation:

$$\Phi(\omega) = \int_{t_s}^{t_m} S(t) \cos[\omega(t - t_0)] dt + A \cdot \int_{\omega^-}^{\omega^+} S(\omega') \frac{\sin [(\omega - \omega')(t_s - t_0)]}{\omega - \omega'} d\omega' + B, \quad (8)$$

where A and B are respectively the scale and offset factor. It is important to note that the correction term has a cardinal sine function $\sin \frac{\alpha x}{x}$ under the integral. In the case where $\alpha = 0$, i.e., $t_s = t_0$, the correction term vanishes. For increasing α values, the correction gets larger in amplitude and more complicated in form and therefore more difficult to deal with. The fit to the data to extract the anomalous precession frequency starts at 30 μ s and thus would be the ideal start time of the fast rotation signal. This scenario is difficult to fulfill due to the beam debunching (there is less frequency information to extract with the increasing start time) and due to the intrinsic limitation of the Fourier method with regard to t_s . For large t_s values, due to the convolution in the integral of the correction term (see eq. (7)) of the approximated frequency distribution $S(\omega')$ and the cardinal sine function, the two terms in eq. (8) interfere and the two distributions merge (see Fig 9). Figure 8 and Fig 9 show the cosine Fourier transform for different t_s values for two different toy Monte Carlo simulations. For more details regarding the Fourier approach and its correction term, refer to [2, 8].

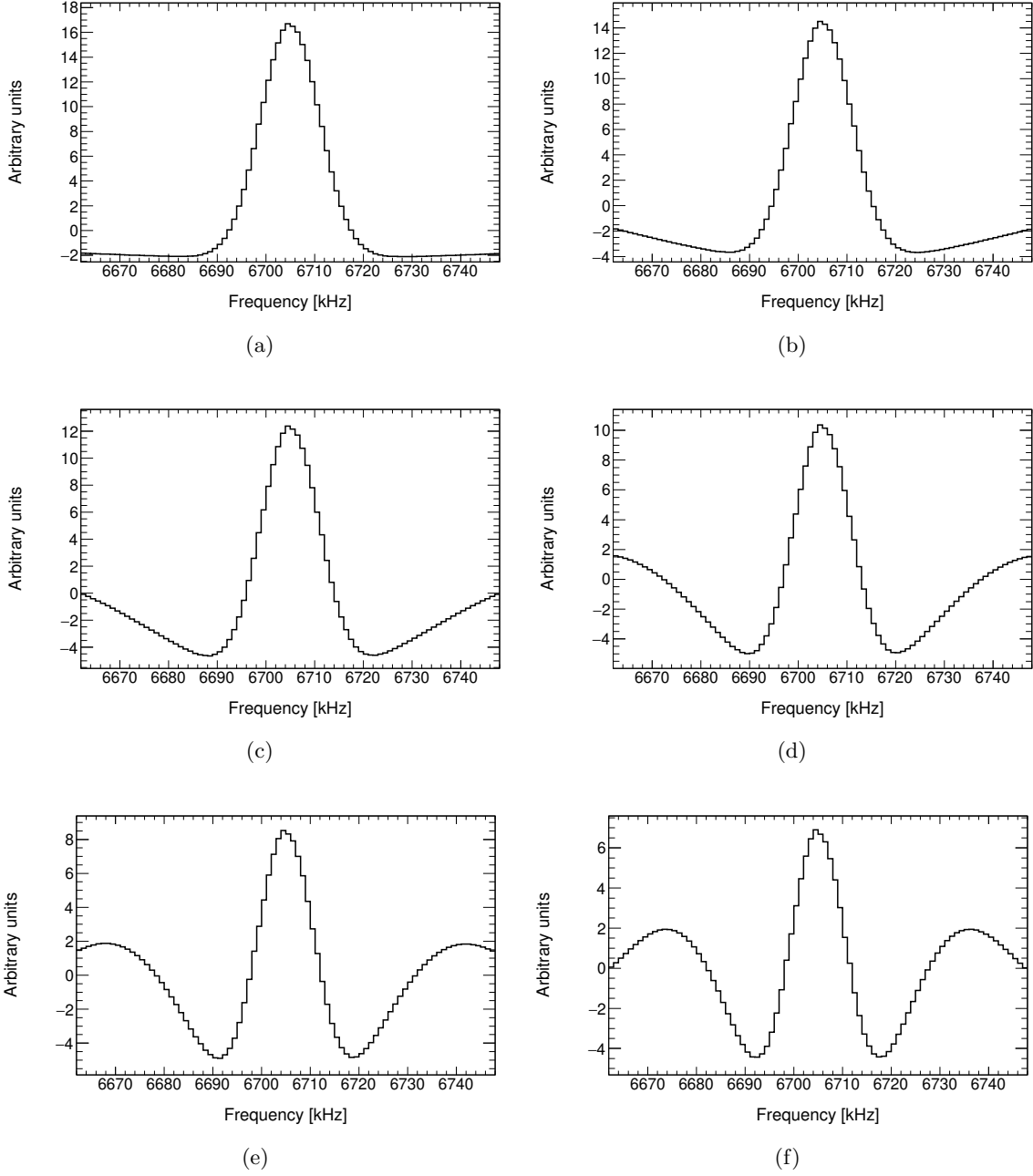


Figure 8: Cosine Fourier transform for: (a) $t_s = 4 \mu$ s, (b) $t_s = 8 \mu$ s, (c) $t_s = 12 \mu$ s, (d) $t_s = 16 \mu$ s, (e) $t_s = 20 \mu$ s, (f) $t_s = 24 \mu$ s with respect to the beam injection. The t_0 parameter is set to the ideal known value for the different t_s configurations. The analyzed fast rotation signal originates from the toy Monte Carlo simulation [3].

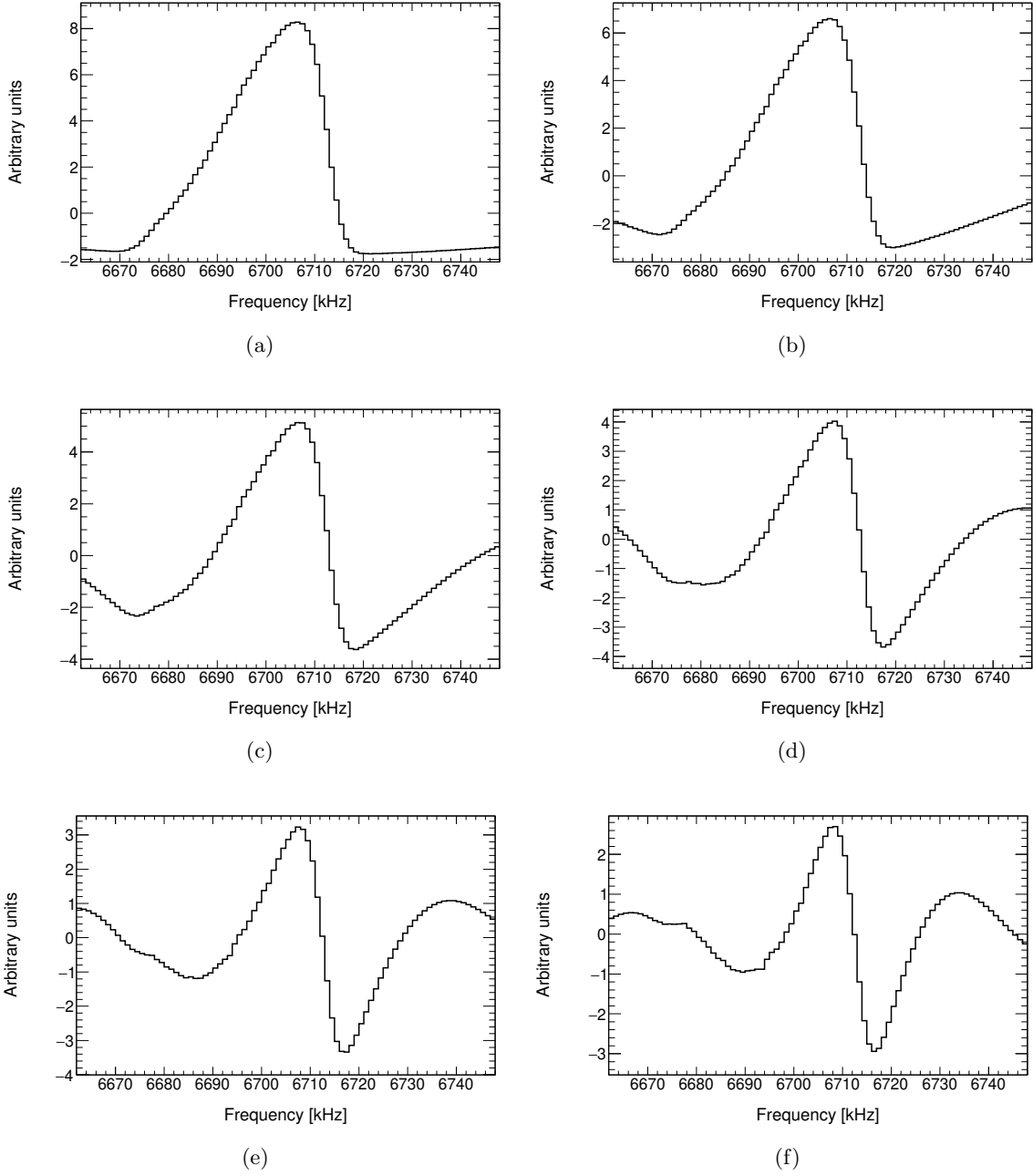


Figure 9: Cosine Fourier transform for: (a) $t_s = 4 \mu s$, (b) $t_s = 8 \mu s$, (c) $t_s = 12 \mu s$, (d) $t_s = 16 \mu s$, (e) $t_s = 20 \mu s$, (f) $t_s = 24 \mu s$ with respect to the beam injection. The t_0 parameter is set to the ideal known value for the different t_s configurations. The analyzed fast rotation signal originates from the toy Monte Carlo simulation [9] that mimics the Run-1 60-hour data set.

5 Background correction

5.1 Signal and background

In the following, when talking about the cosine Fourier transform, the term “signal” refers to the central part of the distribution. It is an approximation of the exact frequency distribution of the stored muons. The term “background” refers to the side bands (tails) of the frequency distribution around the central part. The background is defined by eq. (7) and is divided into two distinct regions. The so-called “physical frequency region” includes only the physical cyclotron revolution frequencies as set by the collimators aperture: 6,662-6,747 kHz. The so-called “non-physical frequency region” includes only the non-physical revolution frequencies, i.e., outside the collimators aperture. The non-physical frequencies are above 6,747 kHz and below 6,662 kHz.

5.2 Background correction

The note [8] shows in details why the background can be well approximated for small t_s values (typically $t_s < 15 \mu s$) by various functions: cardinal sine function, error function, triangle-based function. The approach to correcting for the background relies on fitting for it directly using one of the functions. The default function being used is the cardinal sine function. For large t_s values the cardinal sine function is not a good enough approximation. The triangle-based function is the most general background form and thus the one being used for asymmetric frequency distributions with unknown functional forms, which is the case for the Run-1 data set. Figure 10 and 11 show the background fit for different t_s values for an ideal toy Monte Carlo [3] and for a toy Monte Carlo [9] that mimics the Run-1 data set.

The larger the t_s the more the background exhibits cardinal sine-like features, though the cardinal sine function is only an approximation. For $t_s=4 \mu s$ (i.e. for small enough t_s), a second order polynomial fit performs similarly to the cardinal sine³ (and other functions) given its Taylor expansion about $x = 0$:

$$\text{sinc}(x) = \sum_{k=0}^{\infty} \frac{(-1)^k x^{(2k)}}{(2k+1)!} = 1 - \frac{x^2}{3!} + \frac{x^4}{5!} - \dots \quad (9)$$

The corrected frequency distribution is retrieved by subtracting the fit function to the cosine Fourier frequency distribution. Though the background fit is piece-wise (side-band fit), the correction using it runs through the entire frequency window.

³The background has cardinal sine-like features for any t_s value up to $30 \mu s$. For small enough values of t_s-t_0 , the cardinal sine is widely spread over the frequency range and its Taylor expansion is valid enough over the frequencies range of interest. For increasing t_s values the period of the cardinal sine function decreases and the background exhibits the various characteristics of the cardinal sine function.

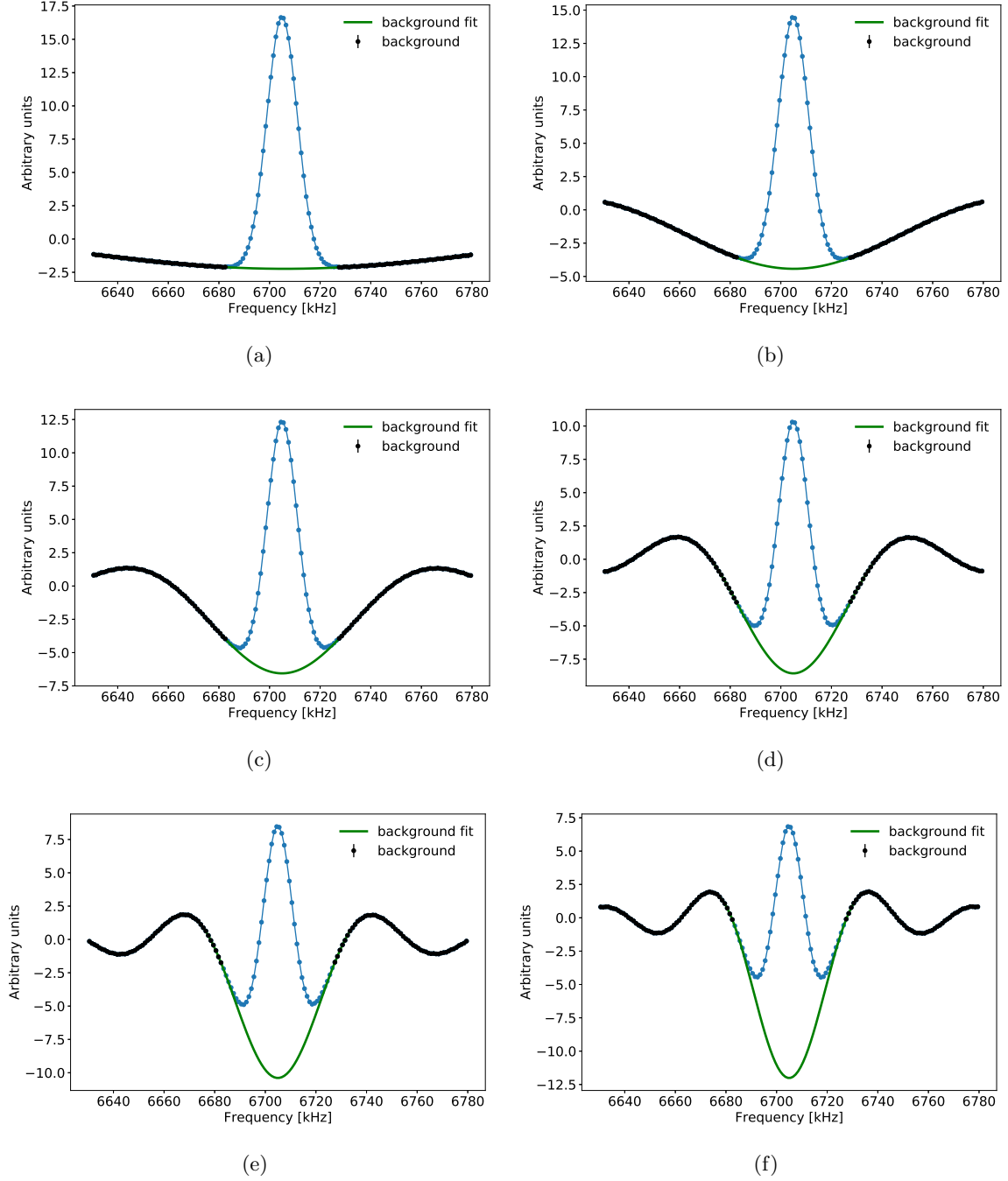


Figure 10: Background fit to the Cosine Fourier transform for: (a) $t_s=4 \mu\text{s}$, (b) $t_s=8 \mu\text{s}$, (c) $t_s=12 \mu\text{s}$, (d) $t_s=16 \mu\text{s}$, (e) $t_s=20 \mu\text{s}$, (f) $t_s=24 \mu\text{s}$. The t_0 value is fixed to the known ideal one for all the t_s configurations. The background fit function is the error function which is the correct form of the background for a Gaussian frequency distribution. The analyzed fast rotation originates from the toy Monte Carlo simulation [3].

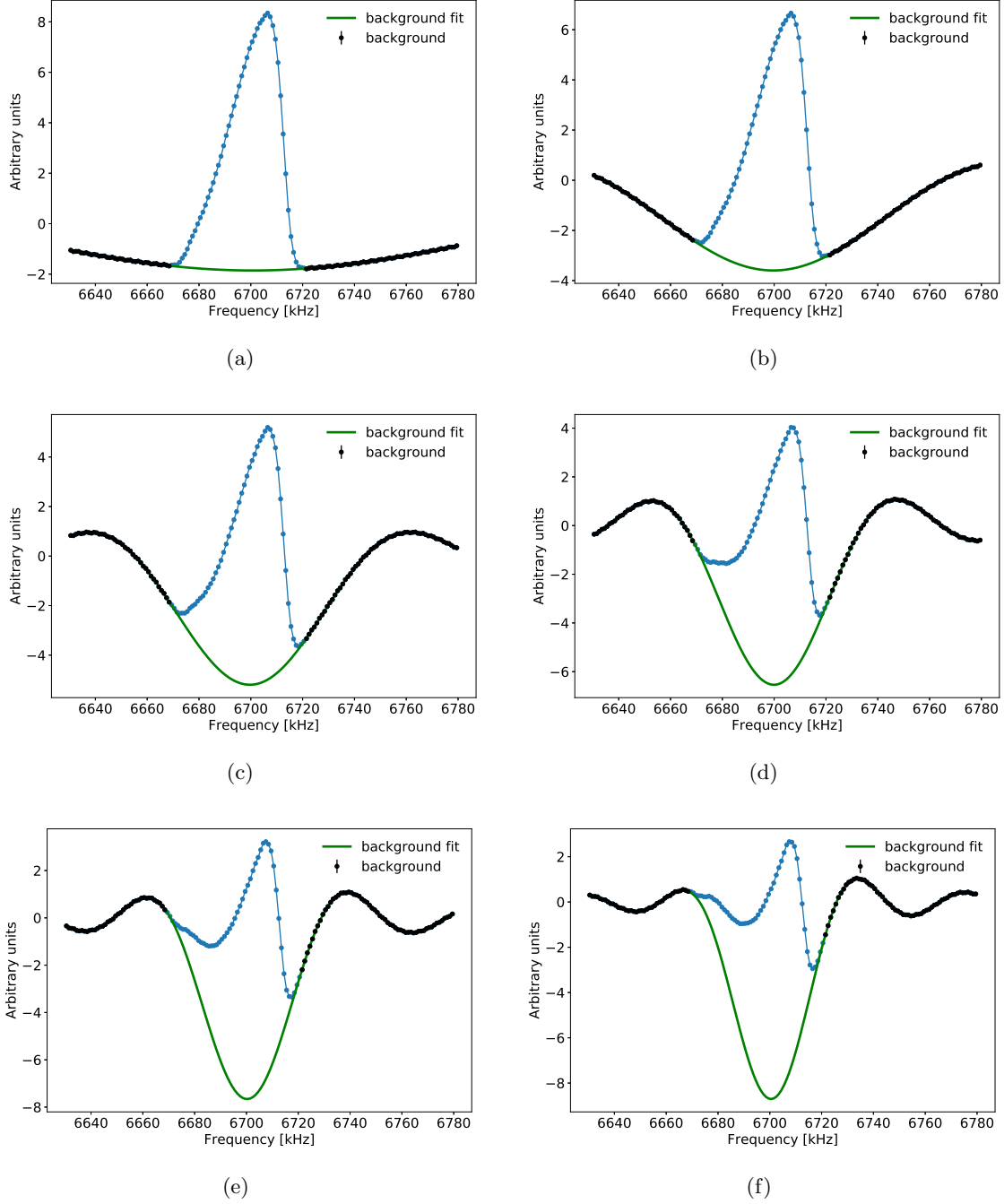
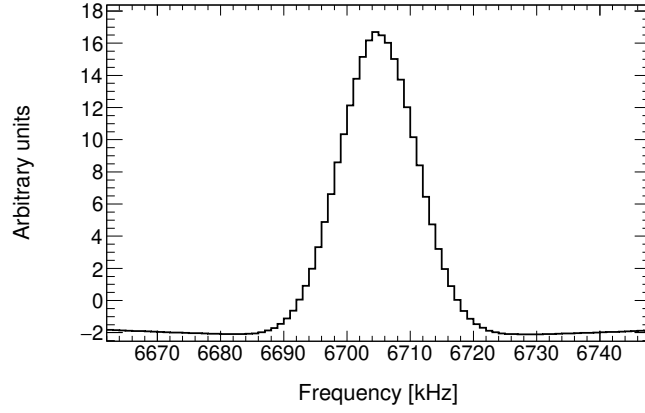


Figure 11: Background fit to the Cosine Fourier transform for: (a) $t_s = 4 \mu s$, (b) $t_s = 8 \mu s$, (c) $t_s = 12 \mu s$, (d) $t_s = 16 \mu s$, (e) $t_s = 20 \mu s$, (f) $t_s = 24 \mu s$. The t_0 value is fixed to the known ideal one for all the t_s configurations. The background fit function is the triangle-based function. The analyzed fast rotation originates from the toy Monte Carlo simulation [9].

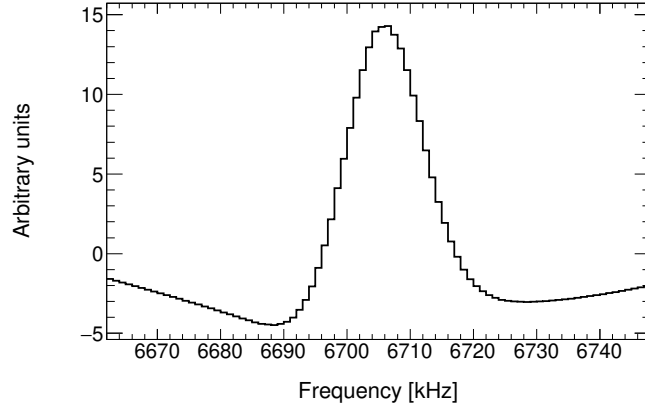
6 t_0 optimization

6.1 Why optimizing?

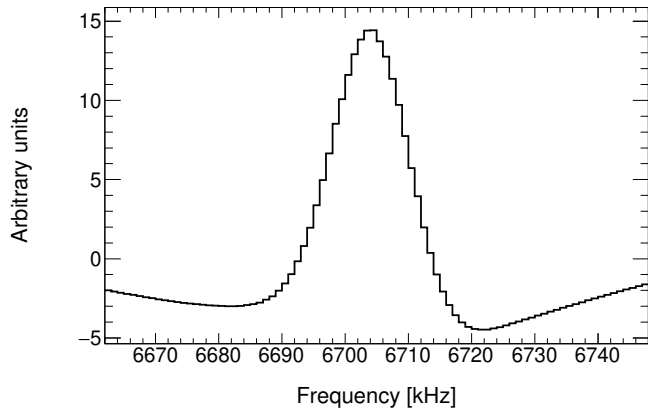
The t_0 parameter corresponds to the center of mass of the beam passing a given detector for the first time (first turn at injection). This parameter cannot be measured directly in the data because of the missing early time data (see Fig. 7). A non-optimum t_0 value leads to distortions in the cosine Fourier transform. Figure 12 shows such distortions for an exaggerated mis-optimization: the cosine Fourier transform is skewed one way or the other causing a bias in the extraction of both its average and width. It is therefore crucial to properly optimize t_0 in order to avoid large systematic uncertainties on the equilibrium radius and width of the beam, and thus the estimation of the electric field correction. Figure 13 shows how much the results change as a function of t_0 given a toy Monte Carlo simulation [9] that mimics the Run-1 data set: a 0.5 ns change in t_0 exceeds the Fermilab E-989 total uncertainty budget on C_E of 20 ppb.



(a)



(b)



(c)

Figure 12: Cosine Fourier transform for three t_0 values: (a) ideal known value, (b) +5 ns t_0 shift, (c) -5 ns t_0 shift. The signal start time is $t_s=8 \mu s$ after the beam injection. The analyzed fast rotation originates from the toy Monte Carlo simulation [3].

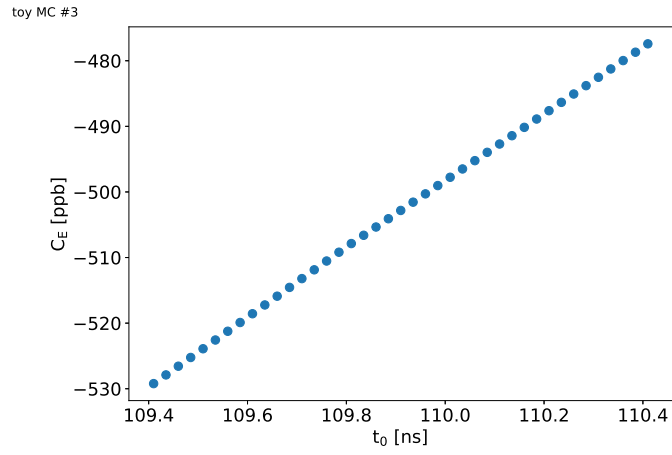
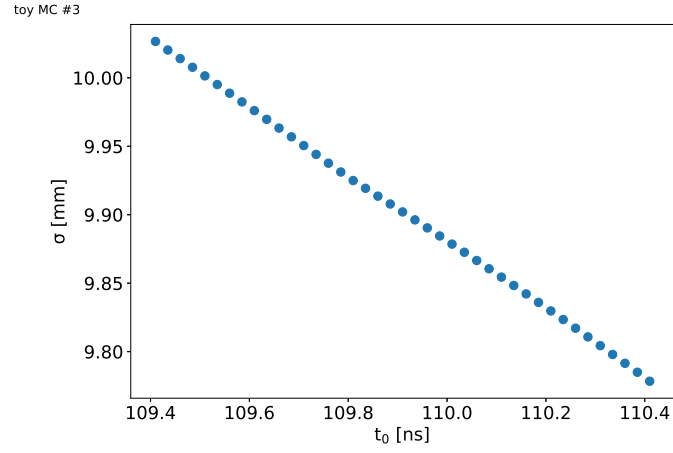
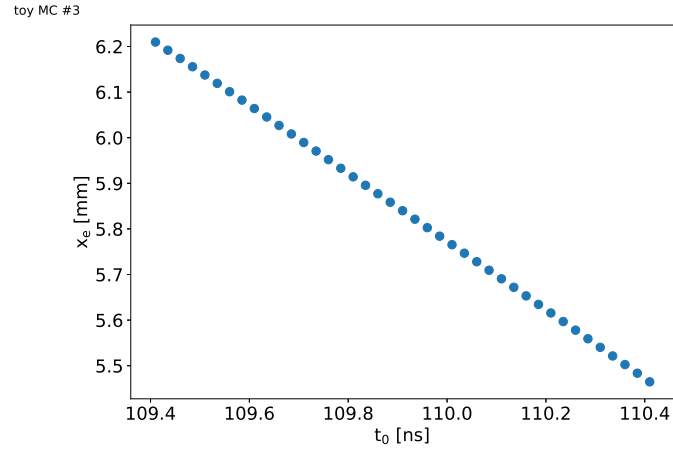


Figure 13: Results of the fast rotation analysis as a function of t_0 for a 1 ns range: (a) equilibrium radius, (b) width, (c) electric field correction. The analyzed fast rotation originates from the toy Monte Carlo simulation [9].

6.2 Optimization procedure

The t_0 optimization procedure is iterative and relies on fitting the background of the cosine frequency distribution with a cardinal sine function. The figure of merit is the χ^2 per degrees of freedom of the background fit. Given the background form is well known for small t_s values, the optimized t_0 value corresponds to the t_0 value that minimizes the χ^2 (given proper modeling, the optimum χ^2 should be 1 when using proper uncertainty on the data point). The nominal frequency window used to fit the background is 6,630-6,780 kHz. The t_s parameter is set to the smallest one possible, thus typically 4 μs in Run-1 data.

6.2.1 First iteration

The cardinal sine fit to the background is performed only in the non-physical frequencies region in order not to make any assumption about the signal and background inside the physical frequency region. The background fit is performed for many t_0 values within a 1 ns range at regular intervals (typically 25 ps). The 1 ns range requires a prior coarse scan to identify at a 1 ns level the optimum t_0 . The uncertainty on each background data point of the cosine frequency distribution σ_{bkg} is set to an initial reasonable guess. For each t_0 value, the fit is performed and the corresponding χ^2 and residuals are computed. From the residuals, the uncertainty on the data point σ_{bkg} is extracted. The optimum t_0 value is defined as corresponding to the minimum χ^2 and the residuals and uncertainty information is saved for the subsequent iterations. Figure 14 shows the results of the first iteration

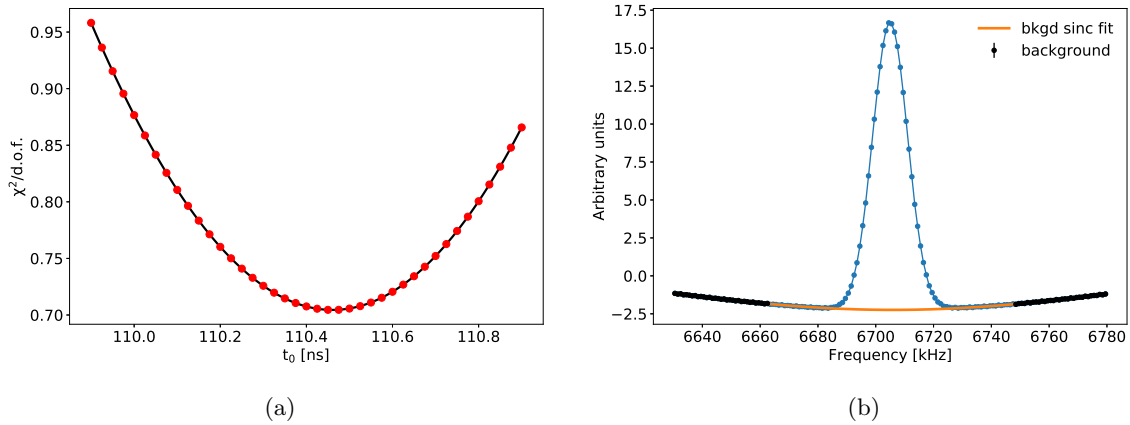


Figure 14: First iteration of the t_0 optimization: (a) χ^2 distribution as a function of t_0 , (b) cosine Fourier transform for the optimal t_0 value corresponding to the minimized χ^2 . The analyzed fast rotation originates from the toy Monte Carlo simulation [3].

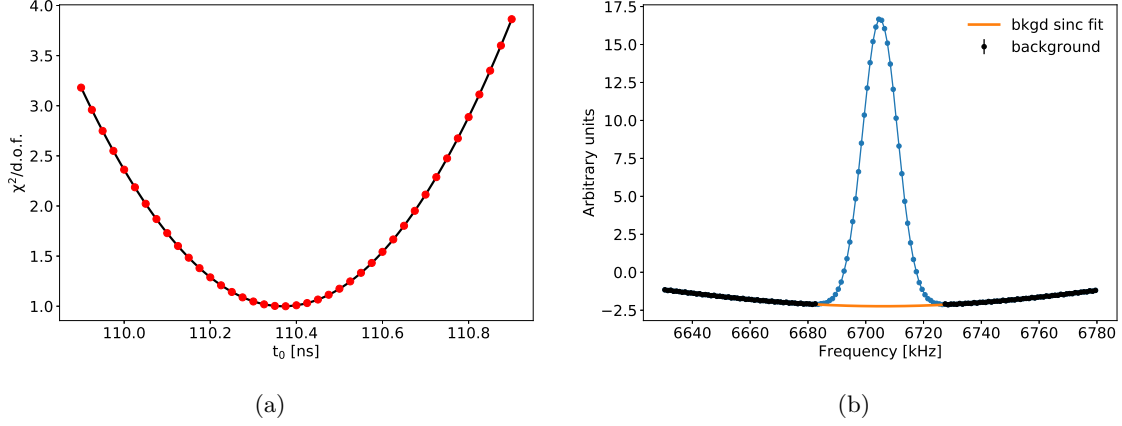


Figure 15: Last iteration of the t_0 optimization: (a) χ^2 distribution as a function of t_0 , (b) cosine Fourier transform for the optimal t_0 value corresponding to the minimized χ^2 . The optimum χ^2 has a value of 1, meaning the background fit model and the uncertainty on the data point are correct. The background region extends into the physical frequency region close to the actual frequency distribution. The analyzed fast rotation originates from the toy Monte Carlo simulation [3].

6.2.2 Next iterations

The background fit is extended to the physical frequencies region in the following fashion: starting from the lower (upper) physical frequency boundary (set by the collimators aperture), data points are added one-by-one to the background if their distance to the optimum background fit from the previous iteration is within $\pm N \cdot \sigma_{bkg}$ where the nominal ⁴ value of N is $N = 2$. The procedure then follows the one detailed for the first iteration. The number of iterations required to reach convergence and a χ^2 of 1 (meaning proper uncertainty estimation) is typically 3 or 4. Figure 15 shows the results of the last iteration (fourth iteration in this case).

⁴There is a systematic uncertainty estimation associated with the choice of N .

7 t_s and t_m optimization

7.1 Spectral leakage

The parameters t_s and t_m also need to be optimized. The first optimization is with respect to each other. The fast rotation signal being of finite length, there is *de facto* a rectangular windowing applied to the data. In order to reduce spectral leakage due to the windowing, t_s and t_m are optimized such as the intensity of the fast rotation signal at t_s and t_m is as close to 1 as possible, i.e., the intensities match each other. For t_s , this translates into an optimized value potentially moved by a quarter of a cyclotron revolution period as seen in Fig. 16. For t_m , because the fast rotation signal has fully debunched and converged to 1 within the statistical noise, this translates into an arbitrary shift.

7.2 t_s optimization

In an ideal world, the data under scrutiny is available from the first turn in the ring, thus $t_s = t_0$ and the cosine Fourier transform of eq. (5) yields the correct answer. But as we have seen for the Run-1 data set, the first few micro-seconds are missing and the muon beam is contaminated by beam-line positrons until about $4 \mu s$. This results in the earliest possible choice for t_s of $4 \mu s$. The t_s optimization is choosing the earliest t_s that corresponds to a stable fast rotation signal. Looking at the analysis results as a function of t_s allows to find

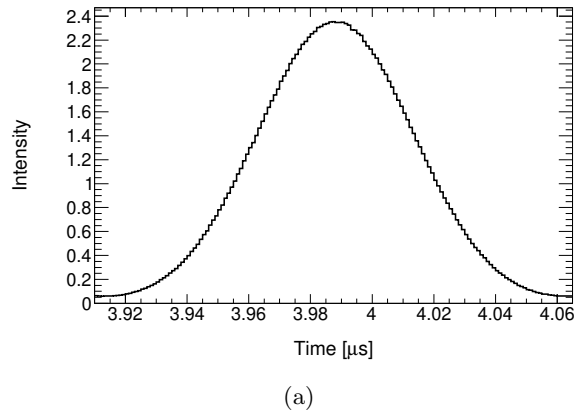


Figure 16: One cyclotron revolution period of the fast rotation signal at $4 \mu s$ after the beam injection. If one chooses $4 \mu s$ by default for t_s , its value will be optimized to the closest value that corresponds to a signal intensity of 1, i.e., $4.022 \mu s$. The maximum optimized shift in t_s corresponds to a quarter of the cyclotron revolution period if t_s is chosen by default to correspond to a maximum or a minimum of the fast rotation signal intensity. The fast rotation signal originates from the toy Monte Carlo simulation [3].

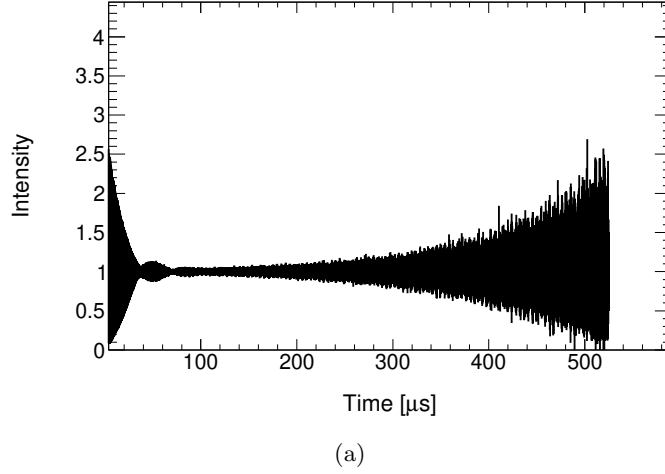


Figure 17: Fast rotation signal of the Run-1 60-hour data set for the time range 4-600 μs after the beam injection.

the earliest t_s value at which the results stabilize (see [10] for more information about the t_s scan). For simulated data, it is very likely that the first turn is available and thus the choice of $t_s = t_0$ is made available⁵.

7.3 t_m optimization

The choice of t_m has to do with the trade off between adding more resolution⁶ to the cosine Fourier transform and adding increasing statistical noise. Figure 17 shows the fast rotation signal for the Run-1 60-hour data set between 4 and 600 μs after the beam injection. The statistical noise clearly blows up passed 400 μs . This blow-up is due to the correction of the exponential muon decay in the positron counts spectrum. The number of counts in the positron counts spectrum is small at late time and thus varies a lot relatively (according to a Poisson distribution).

A rule of thumb approach to approximately choose the proper t_m is to choose t_m as large as possible such as the variation in the intensity of the fast rotation signal does not exceed the band 0.7-1.3, i.e., within 30% of the average intensity. The more statistics a data set has, the later t_m can be chosen. The proper way to optimize t_m is to perform a scan of t_m values and look at how stable the analysis results are (see [10] for more information about the t_m scan).

As stated previously, the range $t_m - t_s$ and the time interval of the fast rotation spectrum

⁵Of course choosing $t_s = 4 \mu s$ in the simulated data allows to mimic the analysis of actual data.

⁶The frequency resolution of the cosine Fourier transform scales as $1/(N_{bin} * T)$ where N_{bin} is the number of bins in the fast rotation histogram and T the time interval between two consecutive bins.

set the frequency resolution. For a typical 4-300 μs time range and a 1 ns time interval, the frequency resolution is $1/(296000 \times 1 \cdot 10^{-9}) = 3.34$ kHz. Performing a fast Fourier transform (FFT) of the fast rotation signal would return a frequency distribution with a frequency bin width of 3.34 kHz. The Fourier analysis of the fast rotation signal relies not on a FFT but on the cosine Fourier transform computation, with the frequency interval left to be chosen. One can thus choose a frequency interval smaller than the frequency resolution, thus over-sampling the frequency distribution. This is what is typically done. This yields to artificial oscillations in the frequency distribution as can be seen in Fig. 18 for an exaggerated case of $t_s = 50 \mu s$. The over-sampling does not cause a shift in the analysis results as discussed in the note [10] Sec. 4.4. Moreover, in order to reconstruct the frequency distribution with enough fidelity, the required frequency interval is below 3 kHz given the frequency distribution is confined within 85 kHz range (collimator aperture) with a typical width of 9 kHz: over-sampling is mandatory.

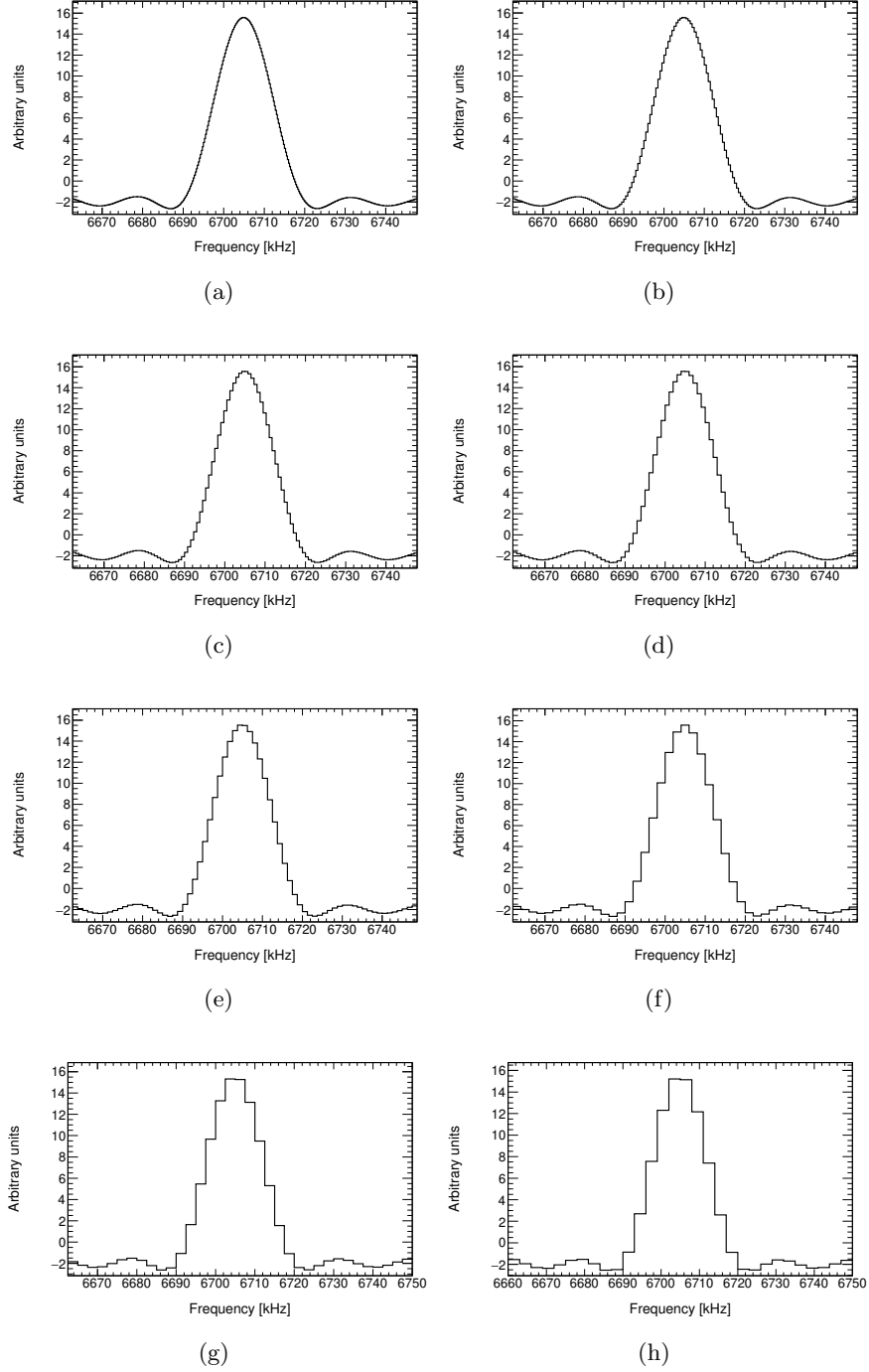


Figure 18: Cosine Fourier transform ($t_s = 4 \mu s$, $t_m = 50 \mu s$) for different frequency intervals: (a) 0.25 kHz, (b) 0.5 kHz, (c) 0.75 kHz, (d) 1 kHz, (e) 1.25kHz, (f) 2 kHz, (g) 2.5 kHz, and (h) 3 kHz. The frequency resolution is 22 kHz which is the period of the observed oscillation. The t_0 parameter is set to the ideal known value. The analyzed fast rotation originates from the toy Monte Carlo simulation [3].

8 Frequency to radius conversion

Once t_0 has been optimized, the cosine Fourier transform can be corrected for the background to retrieve the complete frequency distribution (see Sec. 5). The last step in the procedure is to convert the frequency distribution into the radial distribution. The storage ring is a weak focusing ring with segmented electrostatic quadrupoles operating at low voltage. This yield to an almost constant dispersion function η ⁷ and therefore the trajectory of the stored muons is a circle in good approximation:

$$r = \frac{v}{2\pi f}, \quad (10)$$

where r is the effective radius that takes into account the dispersion function η , f the frequency and v the velocity. The fast rotation analysis provides the information about f . The remaining unknown is v . For a given momentum p , the velocity of a particle of mass m can be retrieved via:

$$p = \gamma m \frac{v}{c}, \quad (11)$$

where c is the speed of light. The γ factor can be computed from:

$$\gamma = \frac{E}{mc^2} = \frac{\sqrt{(mc^2)^2 + (pc)^2}}{mc^2}, \quad (12)$$

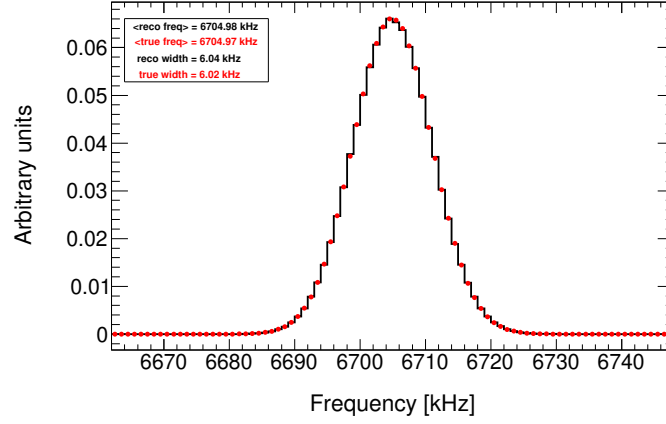
The storage ring has a relative momentum acceptance of about $\pm 0.63\%$. The nominal momentum of the stored muon (the so-called “magic” momentum) is 3.094 GeV/c. This leads to an absolute momentum acceptance of ± 0.02 GeV/c. From eq. (11), the allowed velocity is therefore:

$$v = 299617805 \pm 2234 \text{ m/s}, \quad (13)$$

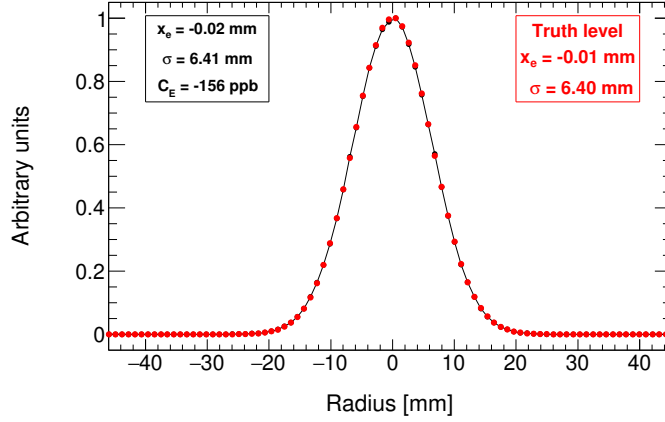
which corresponds to a maximum relative velocity change of $8 \cdot 10^{-6}$. Fixing the value of the velocity to the magic value yields an error on the frequency-radius conversion smaller than 0.05 mm⁸. One could calculate the velocity for each frequency slice using the known dispersion η of the storage ring. In the current context, the introduced uncertainty is small enough to be overlooked. Figure 19 shows an example of a frequency distribution and its radial counterpart.

⁷The dispersion relates the radial offset to the momentum offset $\eta = \frac{\Delta x}{\Delta p/p}$ where Δx is the absolute radial offset and Δp the corresponding absolute momentum offset. The dispersion also relates the radial position x and momentum to the path length C around the ring $\frac{\Delta C}{C} \sim \frac{\eta}{x} \frac{\Delta p}{p}$.

⁸0.05 mm corresponds to the worst case scenario of a muon with a momentum on the edge of the acceptance.



(a)



(b)

Figure 19: Results of the analyzed toy Monte Carlo fast rotation signal [3]: (a) frequency distribution, and (b) the corresponding radial distribution. Are overlaid the truth-level information (red) and the results of the Fourier analysis (black).

9 Performance study and Run-1 data analysis

The performance [10] of the Cornell fast rotation Fourier method has been thoroughly investigated using toy Monte Carlo simulations. Similar studies have started with **BMAD** but will not be the subject of a note for lack of time and people leaving the Cornell group. At the time of writing this note, there is no large statistics simulated sample available from **gm2ringsim** to perform similar performance studies. Both these studies will hopefully be available in a near future.

Various data set from Run-1 have been analyzed with estimation of the statistical and systematic uncertainties: 60-hour [4], 9-day [5], end game [6], high kick [7].

10 Analysis code

The Cornell fast rotation Fourier analysis code is available for download. The user guide [11] provides all the relevant information to download and run the code.

References

- [1] Y. Orlov et al., NIM A 482 (2002) 767-755.
- [2] A. Chapelain, D. Rubin, D. Seleznev, *Extraction of the Muon Beam Frequency Distribution via the Fourier Analysis of the Fast Rotation Signal*, E989 note 130, [GM2-doc-9701](#)
- [3] See ‘TMC #1’ in: [GM2-doc-13759](#)
- [4] A. Chapelain, J. Fagin, D. Rubin, D. Seleznev, *Fast rotation analysis of the Run-1 60-hour data set with the Cornell Fourier method*, [GM2-doc-19150](#)
- [5] A. Chapelain, J. Fagin, D. Rubin, D. Seleznev, *Fast rotation analysis of the Run-1 9-day data set with the Cornell Fourier method*, [GM2-doc-19252](#)
- [6] A. Chapelain, J. Fagin, D. Rubin, D. Seleznev, *Fast rotation analysis of the Run-1 End-game data set with the Cornell Fourier method*, [GM2-doc-19258](#)
- [7] A. Chapelain, J. Fagin, D. Rubin, D. Seleznev, *Fast rotation analysis of the Run-1 High-kick data set with the Cornell Fourier method*, [GM2-doc-COMING-SOON](#)
- [8] A. Chapelain, J. Fagin, D. Rubin, D. Seleznev, *On the background correction of the Cornell fast rotation Fourier method*, [GM2-doc-19925](#)
- [9] See ‘TMC #3’ in: [GM2-doc-13759](#)
- [10] A. Chapelain, J. Fagin, D. Rubin, D. Seleznev, *Performance study of the Cornell fast rotation Fourier analysis with toy Monte Carlo simulations*, [GM2-doc-19132](#)
- [11] A. Chapelain, J. Fagin, D. Rubin, D. Seleznev, *Cornell fast rotation Fourier analysis user guide*, [GM2-doc-18460](#)